

FROM THE DEPARTMENT OF RADIATION PHYSICS, KAROLINSKA INSTITUTET, S-104 01 STOCKHOLM, SWEDEN,
AND THE POLYTECHNIC OF CENTRAL LONDON, LONDON. W1R 8AL, ENGLAND

NEUTRON DOSIMETRY WITH DETECTORS OF FINITE SIZE

II. Experiments and calculations

A. MONTELIUS, T. E. BURLIN and J. BRIGGS

Abstract

In a previous article a theory for detector response in fields of fast neutrons was presented. In the present paper this theory is subjected to experimental tests. For detectors of sizes comparable to the ranges of the neutron produced charged particles the theory predicts the variation of the detector response with detector size and elemental composition of the detector. A tissue-equivalent ionization chamber exposed to a field of ^{252}Cf neutrons was used in the experimental tests of the theory. The size dependence of the response was investigated by varying the chamber gas pressure and the effects of different elemental compositions (mainly hydrogen content) was investigated by using different gases in the chamber (H_2 , CH_4 , TE-gas N_2 , Air, CO_2 , and Ar). The theory was evaluated both by using chord length distributions to characterize the chamber cavity and with a simplified version using a single mean chord length. The agreement between theory and experiment is generally good.

Key words: Neutron dosimetry, finite size detectors, experimental.

In a previous report (12) a theory for detectors in neutron fields was presented. Throughout that article the detector refers to the sensitive volume of the instrument only. The theory was developed for the case of convex detectors exposed to a uniform isotropic field of neutrons. In the present paper the theory is subjected to experimental examination using a tissue equivalent ionization chamber exposed to fission neutrons from a ^{252}Cf source.

Theory predicts that for both very large and very small detectors the specific ionization is constant. It is in the region between these two extremes that the theory predicts the specific ionization varies with detector size and this is the region where the most rigorous test of theory may be applied. The dependence of the response of the ionization chamber on cavity size has been studied by varying the gas pressure. The size of the chamber was

deliberately chosen to cover this intermediate region. Thus most of the charged particles produced in the chamber wall are stopped in the gas at atmospheric pressure, but at the lowest pressures most recoil protons from the wall would cross the chamber. Theory also predicts differences in the ionization chamber response with different atomic composition of the wall and of the gas. A second test of theory has been applied by varying the gas in the chamber. Energy deposition and hence ionization is dominated by the hydrogen content. Therefore gases with different hydrogen components and gases with no hydrogen were employed to test the theory.

The experimental results are compared with theoretical calculations for different cavity shapes and with simplifications of the theory.

Experiment

The experiments were carried out with an ionization chamber with tissue-equivalent (A-150) walls, Landis and Gyr type EQN1, placed in air with its centre at a distance of 50 cm from the ^{252}Cf source. The shape of the chamber, which is shown in Fig. 1, can be described as two half spheres joined by a cylindrical part. The thickness of the chamber wall was 7 mm, which exceeds the range of the most penetrating charged particles produced by the neutrons used in these experiments.

The pressure of the gas in the chamber could be varied from about 3 kPa up to atmospheric pressure. The pressure was reduced by a rotary oil pump, stabilised by a gas reservoir in series with the ionization chamber. The pressure was measured by an open mercury manometer in the

Accepted for publication 18 February 1986.

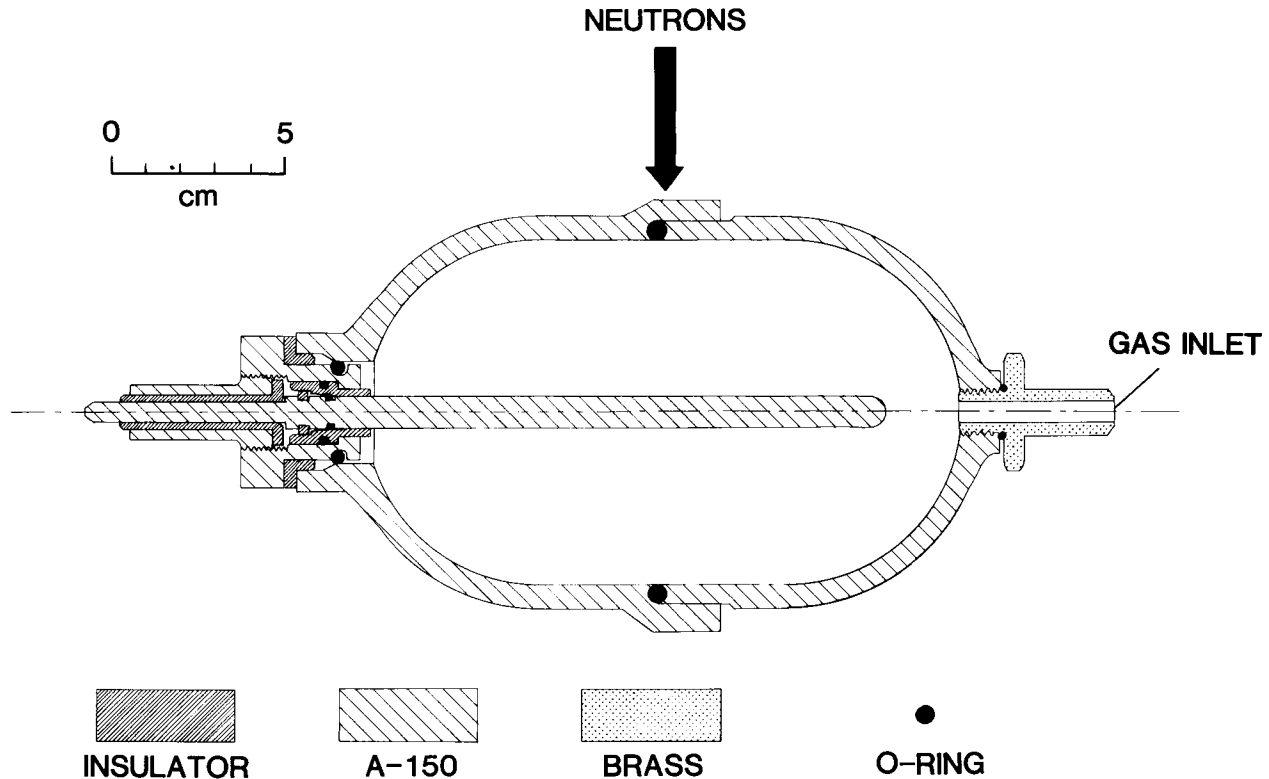


Fig. 1. Tissue-equivalent ionization chamber (Landis and Gyr, type EQN1) which can be operated with different gases at pressures up to atmospheric pressure.

pressure range from 45 to 100 kPa and by a closed mercury manometer below 45 kPa. The gases used were hydrogen, nitrogen, argon, methane, carbon dioxide, air and methane based tissue-equivalent (TE) gas (16).

The ionization was measured with a Vibron 33C electrometer. The measured ionization was corrected for pressure and temperature variations. The collecting voltage was kept at such a level that the recombination was less than 2 per cent.

The ^{252}Cf (Amersham) source gave $2.3 \cdot 10^9$ neutrons per second. The neutron beam was contaminated with γ -rays, which means that the contribution to the mass ionization from γ -rays had to be subtracted to yield the mass ionization due to neutrons only. The ratio of neutron to photon fluence emitted from the source was 0.177 according to the Amersham data sheet. The photon corrections will be described more in detail in the next section.

Photon corrections

The ratio of mass ionization of photons to neutrons J_γ/J_n is given by

$$\frac{J_\gamma}{J_n} = \frac{(D_m)_\gamma}{(D_m)_n} \frac{(\bar{D}_d/D_m)_\gamma}{(\bar{D}_d/D_m)_n} \frac{\bar{W}_n}{\bar{W}_\gamma} \quad (1)$$

where D_m is the equilibrium dose in the chamber wall, \bar{D}_d/D_m is the detector to medium dose ratio defined in part I (12) and \bar{W} is the average energy expended in the gas to form an ion pair. The subscripts γ and n refer to photons and neutrons, respectively.

$(D_m)_\gamma$ is calculated by integrating the product of the differential energy fluence of photons and the mass energy absorption coefficient over all photon energies. The energy spectrum of the γ -rays emitted from the ^{252}Cf source is given by ICRU (8). As the mean γ -ray energy is 0.8 MeV most of the electrons emitted from the chamber wall will cross the chamber even at atmospheric pressure and therefore the fraction of the specific ionization due to photons was treated as constant (i. e. independent of detector size). $(\bar{D}_d/D_m)_\gamma$ or the stopping power ratio was evaluated by using the continuous slowing down approximation (eq. 12 in part I) to calculate the energy distribution of the electrons emitted from the wall (slowing down spectrum). The Compton effect is the dominating photon interaction process for the ^{252}Cf γ -rays and was therefore the only process considered in these calculations. The mass stopping power data of BERGER & SELTZER (1) were used to calculate the slowing down spectrum in the wall material as well as the stopping power ratios. \bar{W}_γ -values for the gases were taken from ICRU (9). The ratio J_γ/J_n

was calculated at atmospheric pressure because it was believed to contain the smallest experimental error. Finally, the specific ionization for neutrons was obtained by subtracting the photon fraction for each gas.

Calculations

Detector shape and irradiation geometry. The geometric shape of the ionization chamber is relatively complex and has therefore been approximated by a geometric form, which is simpler to describe mathematically, namely a sphere, a prolate spheroid and a cylinder both of elongation 1.8. The dimensions of these geometric bodies have been chosen such that their mean chord length, \bar{X}_μ is identical to the mean chord length of the ionization chamber, which is 8.0 cm. The chord length distributions for the sphere, the spheroid and the cylinder are shown in Fig. 2 of part I.

It should be pointed out that the experimental situation does not fulfil the basic assumptions in the theory. The chamber is exposed to a divergent neutron field, while the chord length distributions in the theory have been calculated for a homogeneous, isotropic field of neutrons.

Neutron energy distribution. The energy distribution of the ^{252}Cf neutrons hitting the ionization chamber was not measured. Instead, the formula similar to that given by WATT (18) was used in the calculations, viz.

$$\phi_{E_n}^n = C \cdot \exp(-0.88E_n) \sinh \sqrt{2.0E_n} \quad (2)$$

where E_n is the neutron energy and C is a normalisation constant.

Basic physical data for calculation of energy deposition. As was mentioned in part I the form in which the theory is written makes it possible to introduce simplified calculations. In this part the stopping power ratios and the ratios $\bar{D}_{d,i}/D_{e,q}$ and $\bar{D}_{d,e}/D_d$ which were defined in part I have been evaluated for the charged particles produced by elastic scattering only, while the kerma factor ratio K_d/K_m was evaluated using the kerma factors calculated by CASWELL et coll. (3). These kerma factors include all interaction processes of importance and give more correct results for large detector sizes than kerma factors based on elastic scattering only would give.

The initial spectra in A-150 and the different gases were calculated using the elastic scattering cross section data from the Evaluated Nuclear Data Files ENDF-B as provided by the OECD data bank (5).

The stopping power and range data of OLDENBURG & BOOZ (14) were used for the calculation of charged particle spectra and energy deposition by charged particles. Their data cover the energy range of charged particles produced by neutrons of energies below 6.5 MeV. The upper neutron energy limit in the present dose calculation was 10 MeV and therefore the tables were extended using the formulas given by OLDENBURG & BOOZ. The stopping

power and range tables for A-150 were recalculated using the elemental composition given by ICRU (8) which is slightly different from the composition given by OLDENBURG & BOOZ. For protons in Ar stopping power and range data from JANNI (10) were used.

W-values. A general review of data for W -values has been published in ICRU (9). It is still difficult to find measured W -values for all types of charged particles in the gases used in this work. Especially for hydrogen the data are very sparse. The value given in ICRU (9) for α -particles was therefore used for all types of charged particles.

The $W(E)$ data for H, C, N and O recoils given by BICHSEL & RUBACH (2) for TE-gas, CO_2 and air were used in the present calculations. For F and Ca-recoils from the chamber wall the values for O recoils were used. The following method presented by BICHSEL & RUBACH (2) to obtain analytic functions for $W(E)$ was used for the gases N_2 , Ar and CH_4 . The experimental values of $W(E)$ were plotted against $\ln(E)$, E and $1/E$. Segments in the different plots were approximated by least square fitted straight lines. Thus $W(E)$ could be represented over the whole measured energy range by simple functions of E .

For energies below the measured data logarithmic extrapolations were used (cf. 6). For energies above the measured range a constant value equal to the value obtained at the highest measured energy was used. Table 1 gives the W -functions for H_2 , N_2 , Ar and CH_4 as well as the references on which they are based.

The homogeneous case

According to Fano's theorem when medium and detector are of identical elemental composition, a theory for detector response should give a detector to medium dose ratio, which is independent of detector size. This homogeneous case was simulated by calculating the detector to medium dose ratio, \bar{D}_d/D_m , (eq. 24 in part I) for a spherical detector filled with a gas of the same atomic composition as A-150 plastic and situated in a A-150 medium exposed to ^{252}Cf neutrons. The results are shown in Fig. 2 where the detector to medium dose ratio is plotted versus detector size, which here is expressed in terms of mean chord length, \bar{X}_μ , of the detector.

In Fig. 2 are also indicated the dose contributions from internal and external particles as well as the contributions from each type of charged particle recoil. The contributions from external and internal particles compensate so that the dose in the detector is constant independent of detector size. It can also be seen that this is the case for each type of charged particle. The effects of charged particle range is clearly demonstrated here. The cross over point, where the contributions from external and internal particles are identical occurs for protons at a detector size, which is about 100 times larger than for calcium recoils.

Table 1
Average energy expended per ion pair formed in different gases

Gas	Ion	$W(E)$ (eV)	Energy range (MeV)	Reference
Methane	H ⁺	$W(E)=30.0$	All energies	13
	C ⁺	$W(E)=-12.37 \ln E+13.9$	<0.07	
		$W(E)=0.805 1/E+35.5$	0.07-0.23	13
		$W(E)=39.0$	>0.23	
	N ⁺	as C ⁺	-	
	O ⁺	$W(E)=14.24 \ln E+13.7$	<0.075	
		$W(E)=0.924 1/E+38.9$	0.075-0.4	13
		$W(E)=41$	>0.4	
F ⁺	as O ⁺	-		
Ca ⁺	as O ⁺	-		
Nitrogen	H ⁺	$W(E)=9.7 E+34.4$	<0.23	13
		$W(E)=36.5$	≥0.23	9
	C ⁺	as N ⁺	-	
	N ⁺	$W(E)=-28.7 \ln E-27.8$	<0.05	11, 13
		$W(E)=0.927 1/E+40.3$	≥0.05	11, 13
	O ⁺	$W(E)=-30.0 \ln E-26.7$	<0.05	11, 13
		$W(E)=1.14 1/E+41.6$	≥0.05	
	F ⁺	as O ⁺	-	
Ca ⁺	as O ⁺	-		
Ar	H ⁺	$W(E)=27.1$	All energies	4, 15
		$W(E)=-42.0 \ln E-99.7$	<0.025	15
	C ⁺	$W(E)=0.543 1/E+33.5$	0.025-0.05	15
		$W(E)=1.192 1/E+21.6$	0.05-0.17	15
		$W(E)=-6.94 E+29.7$	0.17-0.6	
	N ⁺	$W(E)=25$	>0.6	
		$W(E)=-42.0 \ln E-96.1$	<0.02	15
		$W(E)=0.748 1/E+32.3$	0.02-0.05	11
	O ⁺	$W(E)=1.34 1/E+20.6$	0.05-0.17	
		$W(E)=-6.94 E+29.7$	0.17-0.6	
		$W(E)=25$	>0.6	
	F ⁺	$W(E)=-42.0 \ln E-84.9$	<0.025	15
		$W(E)=1.01 1/E+30.3$	0.025-0.045	11
		$W(E)=1.28 1/E+23.8$	0.045-0.17	
	Ar ⁺	$W(E)=-11.32 E+33.0$	0.17-0.5	
		$W(E)=27.0$	>0.5	
		as O ⁺	-	
	Ca ⁺	$W(E)=-29.36 \ln E-17.5$	0.035	4, 15
$W(E)=-17.2 \ln E+23.6$		0.035-0.33		
$W(E)=42$		>0.33		
Hydrogen	H ⁺	$W(E)=36.4$	All energies	9
	all other	as H ⁺	-	-

For the TE-gas used in the chamber (and for all other gases) the match between the atomic composition of the gas and the wall was not perfect. Therefore the particle types do not compensate and there is some size dependence of the response.

Results and Discussion

The experimental results from the ionization chamber measurements with the different gases are shown in Fig. 3

together with the curves calculated for a spherical chamber. The experimental points for all gases have been normalized to the calculated value for TE-gas at atmospheric pressure. TE-gas was chosen as reference gas because it is a gas used in standard dosimetry and the stopping power and W -data are probably less uncertain for this gas than for most other gases. It is also an advantage that the chamber response with this gas varies very little with pressure.

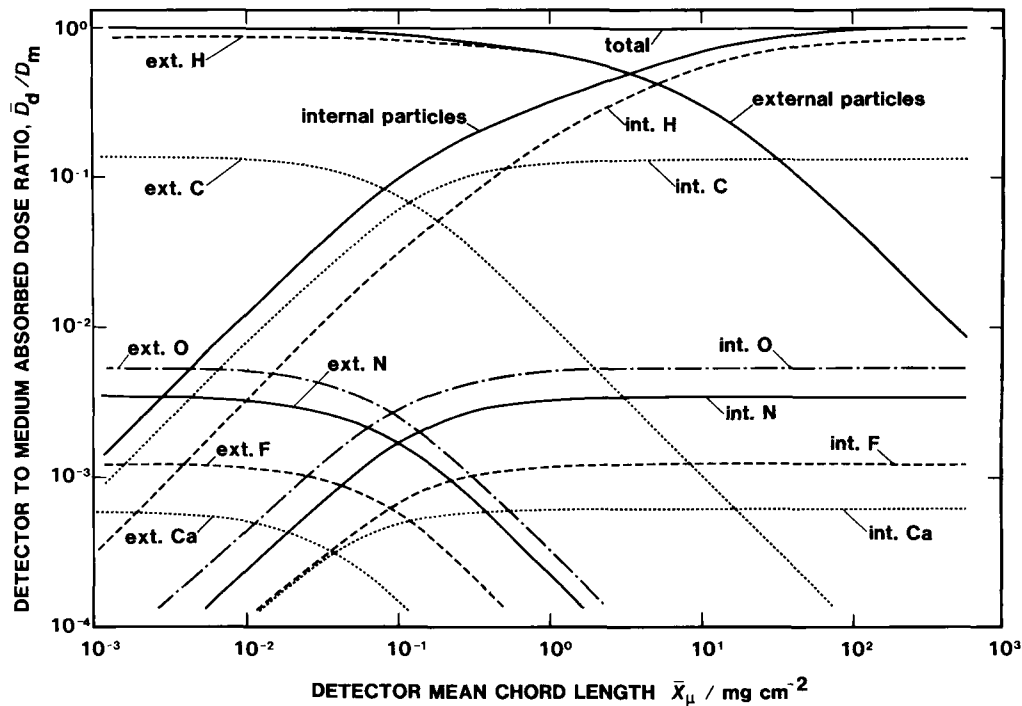


Fig. 2. Dose conversion factor and fractional contributions from external and internal charged particles as a function of detector size for a homogeneous spherical A-150 detector. The detector

size is expressed in terms of mean chord length, \bar{X}_μ , for the detector.

A detailed error analysis will not be presented here, but the total error in the experimental points ($\pm 10\text{--}12\%$) has been estimated and is indicated in the figures. The main sources of error are lack of saturation in the ion collection, errors in chamber gas pressure readings, especially at low pressures and also errors in the separation of mass ionization from photons and neutrons. The latter error is estimated to contribute by approximately 50 per cent to the total error. Uncertainties of the same order also arise in the theoretic calculations from the basic physical data selected and possibly also from neglecting any neutrons scattered in the room.

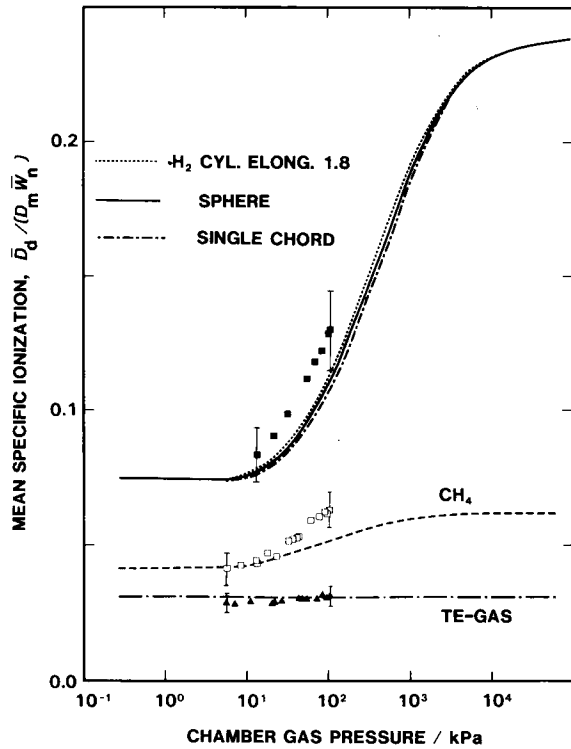
The agreement between theory and experiment is generally fair. The dependence of the specific ionization on cavity size (gas pressure) has been clearly demonstrated. This conflicts with the independence predicted by the earliest cavity theory for neutrons (7) but concurs with the dependence predicted by the present theory and other more recent theoretical treatments (e.g. 17). Furthermore, the direction of that dependence for different cavity gases has been correctly predicted.

Both hydrogen and methane have a larger hydrogen content than the wall material, A-150. As the gas pressure increases the internal proton recoils from elastic scattering in hydrogen will become more and more important and consequently the chamber response will increase. This can be seen in both theory and experiment, but the increase in the experimental points is larger than in the

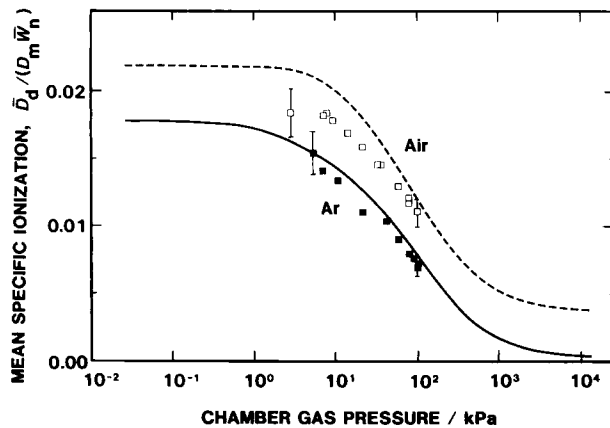
theoretical curves, especially for methane. Even for TE-gas the experiment shows a small increase with pressure, which is not reflected in the calculated curve.

The agreement between theory and experiment is better for the hydrogen free gases, especially for argon and carbon dioxide. Both theory and experiment show a decrease in ionization with gas pressure, which is caused by the fact that the protons from the chamber wall are stopped in the gas but not compensated by protons produced in the cavity. The ionization is therefore predominantly produced by protons generated in the wall. The slope in the theoretical curves for nitrogen and air, which is 76 per cent nitrogen, is steeper than the experiment. This may in part be caused by the omission of the (n, p)-reaction in nitrogen in the calculation.

For hydrogen and carbon dioxide the theoretical curves for the cylinder of elongation 1.8 are also shown. For cavity sizes comparable to the ranges of the charged particles the ionization in the cylinder is larger than the ionization in a sphere with the same mean chord length. This is caused by the fact that the cylinder has a number of chord lengths, which are much longer than the maximum chord length of the sphere, and a relatively large amount of energy is deposited along these long chords. The results for the prolate spheroid were almost identical to those of a sphere and they are therefore not included in the figures. The differences caused by geometric shape are comparatively small. However, in a parallel beam of



a

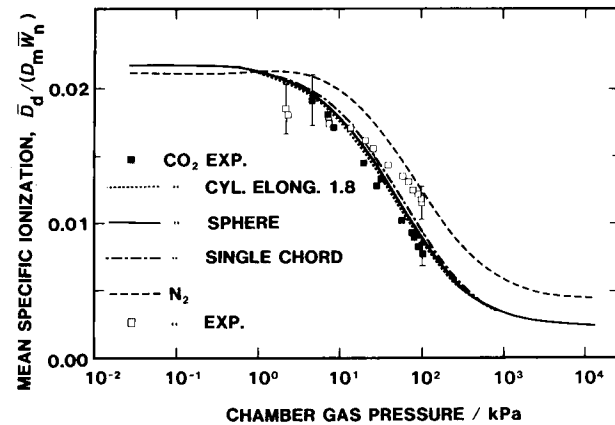


c

neutrons the differences can be larger and the directional dependence may therefore not be negligible.

The results of calculations with the simplified model using a single mean chord length for the external particles are also shown in Fig. 3 for hydrogen and carbon dioxide. The difference between the curves calculated with this simplified model and the curves obtained with distributions for sphere and cylinder is small, indicating that this simplification is a useful approximation.

In Table 2 the dependence of the specific ionization of the gas in the cavity is compared for theory and experiment. Both the theoretical and the experimental values have been normalized on the values for tissue equivalent



b

Fig. 3. Experimental and calculated relative ionization per unit mass (in units of $(\bar{D}_d/D_m)\bar{W}_n$) as a function of gas pressure in the ionization chamber.

Table 2

Comparison of experimental measurements and theoretical calculations of the specific ionization in different gases

Pressure	6.7 kPa		101.3 kPa	
	Theory	Experiment	Theory	Experiment
TE	1.00	1.00	1.00	1.00
Air	0.657	0.676	0.385	0.357
Ar	0.529	0.502	0.251	0.222
N ₂	0.632	0.663	0.399	0.373
CO ₂	0.646	0.608	0.283	0.248
H ₂	2.82	2.43	3.54	4.18
CH ₄	1.46	1.36	1.65	2.03

gas at 6.7 kPa and at 101.3 kPa. There are two main sources of uncertainty in this comparison, namely the value of the average energy expended in the gas per ion pair formed (particularly for hydrogen) and also the magnitude of the photon component to be subtracted from the ionization. The agreement between theory and experiment is good for the hydrogen-free gases but differences of about 20 per cent occur for the hydrogen-rich gases.

Conclusion

The present approach to describe energy deposition in detectors of any size agrees for the most part with experiment within the error limits, though the errors both in experiment and theory are larger than for photon fields. The general tendencies of the curves of ionization versus detector size for the different chamber gases are well explained by the theory.

As discussed in part I (12) the mathematical form in which the theory is expressed, enables simplifications to be made, which may be of interest in many practical situations.

The agreement between theory and experiment encourages the application of the theory to other problems, such as the response of other neutron detectors or to the dosimetry of bone in neutron fields.

ACKNOWLEDGEMENTS

The valuable discussions with Dr A. Brahme are gratefully acknowledged. This investigation has in part been supported by a grant from Cancerföreningen in Stockholm.

Request for reprints: Dr Anders Montelius, Department of Radiation Physics, Karolinska Institutet, P.O. Box 60204, S-104 01 Stockholm, Sweden.

REFERENCES

1. BERGER M. J. and SELTZER S. M.: Stopping power and ranges of electrons and positrons. National Bureau of Standards, Washington, DC, NBSIR 82-2550, 1982.
2. BICHSEL H. and RUBACH A.: Neutron dosimetry with spherical ionisation chambers. II. Basic physical data. *Phys. Med. Biol.* 27 (1982), 1003.
3. CASWELL R. S., COYNE J. J. and RANDOLPH M. L.: Kerma factors for neutron energies below 30 MeV. *Radiat. Res.* 83 (1980), 217.
4. CHEMTOB M., PARMENTIER N. and NGUYEN V. D.: Some experimental results on W -values for heavy particles. *Phys. Med. Biol.* 23 (1978), 1197.
5. ENDF-B4. Evaluated nuclear data files. Brookhaven National Laboratory. (OECD, data bank, Gif-sur-Yvette.)
6. GOODMAN L. J. and COYNE J. J.: W_n and neutron kerma for methane-based tissue-equivalent gas. *Radiat. Res.* 82 (1980), 13.
7. GRAY L. H.: The ionization method of measuring neutron energy. *Proc. Cambr. Phil. Soc.* 40 (1944), 72.
8. ICRU Report No. 26. Neutron dosimetry for biology and medicine. International Commission on Radiation Units and Measurements, Washington, DC 1977.
9. ICRU Report No. 31: Average energy required to produce an ion pair. International Commission on Radiation Units and Measurements, Washington, DC 1979.
10. JANNI J. F.: Calculations of energy loss, range, pathlength, straggling, multiple scattering and the probability of inelastic nuclear collisions for 0.1 to 1000 MeV protons. Technical Report No. AFWL-TR-65-150. Air Force Weapons Laboratory, New Mexico, 1966.
11. LEIMGRUBER R., HUBER P. U. und BAUMGARTNER E.: Messung der Arbeit pro Ionenpaar in verschiedenen Gasen für Stickstoff- und Sauerstoffionen im Energiegebiet von 0,14 bis 0,7 MeV. *Helv. Phys. Acta* 38 (1965), 499.
12. MONTELIUS A.: Neutron dosimetry with detectors of finite size. I Theory. *Acta radiol. Oncology* 25 (1986), 295.
13. NGUYEN V. D., CHEMTOB M., CHARY J., POSNY F. and PARMENTIER N.: Recent experimental results on W -values for heavy particles. *Phys. Med. Biol.* 25 (1980), 509.
14. OLDENBURG V. and BOOZ J.: Mass stopping power and path length of neutron produced recoils in tissue and tissue equivalent materials. Euratom Biology Service CCR, Ispra, Italy. EUR 4876, 1972.
15. PHIPPS J. A., BORING J. W. and LOWRY R. A.: Total ionization in argon by heavy ions of energies 8 to 100 keV. *Phys. Rev.* 135 (1965), 36.
16. ROSSI H. H. and FAILLA G.: Tissue equivalent ionization chambers. *Nucleonics* 14 (1956), 32.
17. RUBACH A. and BICHSEL H.: Neutron dosimetry with spherical ionisation chambers. I. Theory of the dose conversion factors r and W_n . *Phys. Med. Biol.* 27 (1982), 893.
18. WATT B. E.: Energy spectrum of neutrons from thermal fission of ^{235}U . *Phys. Rev.* 87 (1952), 1037.